

Review

Research on Silicon-Substrate-Integrated Widely Tunable, Narrow Linewidth External Cavity Lasers

Xuan Li, Junce Shi, Long Wei, Keke Ding, Yuhang Ma, Zaijin Li *, Lin Li, Yi Qu, Zhongliang Qiao, Guojun Liu and Lina Zeng

Key Laboratory of Laser Technology and Optoelectronic Functional Materials of Hainan Province, Academician Team Innovation Center of Hainan Province, College of Physics and Electronic Engineering, Hainan Normal University, Haikou 571158, China; lixuan13025794412@163.com (X.L.); jcs1075106215@163.com (J.S.); weilong0096@163.com (L.W.); dingkeke1205@163.com (K.D.); mayuhang327@163.com (Y.M.); licust@126.com (L.L.); quyihainan@126.com (Y.Q.); qzhl060910@hainnu.edu.cn (Z.Q.); gjliu626@126.com (G.L.); zenglinahainan@126.com (L.Z.)

* Correspondence: lizaijin@126.com

Abstract: Widely tunable, narrow linewidth external cavity lasers on silicon substrates have many important applications, such as white-light interferometry, wavelength division multiplexing systems, coherent optical communication, and optical fiber sensor technology. Wide tuning range, high laser output power, single mode, stable spectral output, and high side-mode suppression ratio external cavity lasers have attracted much attention for their merits. In this paper, two main device-integrated structures for achieving widely tunable, narrow linewidth external cavity lasers on silicon substrates are reviewed and compared in detail, such as MRR-integrated structure and MRR-and-MZI-integrated structure of external cavity semiconductor lasers. Then, the chip-integrated structures are briefly introduced from the integration mode, such as monolithic integrated, heterogeneous integrated, and hybrid integrated. Results show that the silicon-substrate-integrated external cavity lasers are a potential way to realize a wide tuning range, high power, single mode, stable spectral output, and high side-mode suppression ratio laser output.

Keywords: silicon substrate; narrow linewidth; widely tunable; external cavity



Citation: Li, X.; Shi, J.; Wei, L.; Ding, K.; Ma, Y.; Li, Z.; Li, L.; Qu, Y.; Qiao, Z.; Liu, G.; et al. Research on Silicon-Substrate-Integrated Widely Tunable, Narrow Linewidth External Cavity Lasers. *Crystals* **2022**, *12*, 674. <https://doi.org/10.3390/cryst12050674>

Academic Editor: Arcady Zhukov

Received: 31 March 2022

Accepted: 6 May 2022

Published: 8 May 2022

Publisher's Note: MDPI stays neutral with regard to jurisdictional claims in published maps and institutional affiliations.



Copyright: © 2022 by the authors. Licensee MDPI, Basel, Switzerland. This article is an open access article distributed under the terms and conditions of the Creative Commons Attribution (CC BY) license (<https://creativecommons.org/licenses/by/4.0/>).

1. Introduction

Silicon-substrate-integrated narrow linewidth tunable external cavity semiconductor lasers (SINLT-ECSLs) are devices composed of the substrates Si, SiO₂, Si₃N₄, or other containing Si materials and external optical feedback elements (low-loss waveguide, waveguide filter, or other elements). By adjusting the external cavity elements, such as polarizer, prism, gratings, etc., narrow linewidth and wide tuning range can be achieved. SINLT-ECSLs have the characteristics of tunable [1], narrow, or even ultra-narrow linewidth [2,3], low noise [4,5], wide application, and so on. In this paper, the device-integrated structures, chip-integrated structures of silicon-based external cavity semiconductor lasers are introduced, and, especially, the integration technology and development are introduced. Silicon-based external cavity semiconductor lasers have significant advantages over Littow and Littman configurations of the external cavity semiconductor lasers in terms of structure design, function types, and application range. In recent years, with the continuous development of optical fiber communication, coherence technology, and other fields, the silicon substrate external cavity semiconductor laser will be applied in more and more fields, with its unique characteristics, and will become the ideal light source.

2. Principle of SINLT-ECSLs

SINLT-ECSLs mainly include a semiconductor optical amplifier (SOA) and a silicon photonic chip, which are integrated through a spot size converter (SSC). An SOA is an

optoelectronic device that, under suitable operating conditions, can amplify an input light signal. A schematic diagram of a basic SOA is shown in Figure 1. The active region in the device imparts gain to an input signal. An external electric current provides the energy source that enables gain to take place. An embedded waveguide is used to confine the propagating signal wave to the active region. When the light signal passes through the active region, it will cause these electrons to lose energy in the form of photons and return to the ground state. The excited photon has the same wavelength as the optical signal; thereby, the optical signal is amplified.

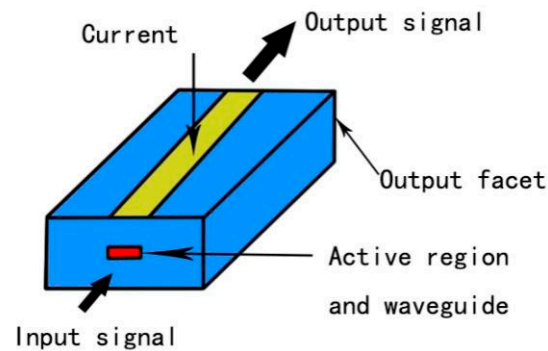


Figure 1. Schematic diagram of an SOA.

The role of the SOA is to provide gain amplification, while the silicon photonic chip is mainly for wavelength selection. Figure 2 shows the typical structure of a silicon-based external cavity semiconductor laser. The light wave of the SOA coupled to the silicon wire waveguide is filtered through two microring resonators (MRR). Two microring resonators with different radii are designed. According to Formula (1), the free spectral range (FSR) is also different due to the different radii of the microring resonators.

$$\text{FSR} = \lambda^2 / 2\pi r n_{\text{eff}} \quad (1)$$

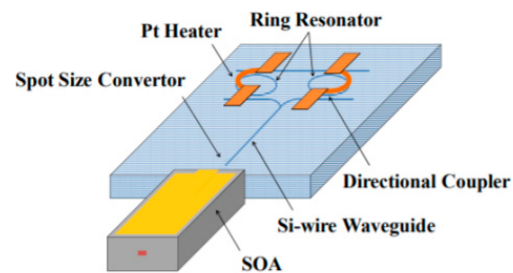


Figure 2. Typical structure of silicon substrate external cavity semiconductor laser.

In Formula (1), the wavelength of the light wave is λ , the radius of the microring resonator is r , and the effective refractive index of the waveguide is n_{eff} . The transmission spectra of the two microring resonators are superimposed on each other, and the wavelength of the mutually matched peak is determined by mode competition. The free spectral range of the microring resonator is changed by adjusting the heater through thermo-optic effect, and the transmission peak moves. The wavelength is tuned through the Vernier effect.

Figure 3 shows the working principle of wavelength tuning of a silicon-based external cavity semiconductor laser. When passing through two annular resonators with different radii, the wavelength difference of resonance results in a Vernier effect. The tuning wavelength range is determined by the radius difference between the two ring resonators. A small radius difference provides a wide wavelength-tuning range, although the transmittance difference between the main peak and the side peak adjacent to the main peak may be small. However, by heating one of the two ring resonators, the peak wavelength of the

transmission spectrum of the dual-ring resonator filter changes discretely according to the resonant wavelength of the other ring resonator filter [6].

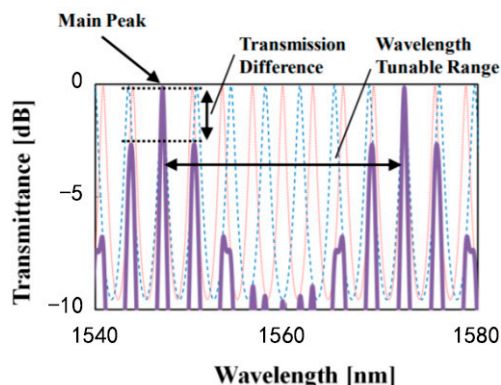


Figure 3. Working principle of wavelength tuning of silicon substrate external cavity semiconductor laser.

3. Research Progress of SINLT-ECSLs

SINLT-ECSLs can be mainly divided into the external cavity semiconductor lasers integrated with a microring resonator (MRR) [7–9], the external cavity semiconductor lasers integrated with an MRR and Mach–Zehnder interferometer (MZI), and the external cavity semiconductor lasers integrated with an MRR and others [10,11]. In order to subdivide it, MRR-integrated external cavity semiconductor lasers can be divided into double-MRR, three-MRR, and multiple-MRR integration. This paper mainly discusses the research progress of double-MRR integration and MRR-and-MZI-integrated external cavity semiconductor lasers.

3.1. MRR-Integrated External Cavity Semiconductor Laser

In 2006, Masahige Ishizaka et al. [12] reported an external cavity semiconductor laser integrated with SiO₂ dual MRR and SOA. The structure is shown in Figure 4, and the wavelength-tuning range is 45 nm, which can completely cover the C-band and L-band in a wavelength division multiplexing (WDM) optical communication system.

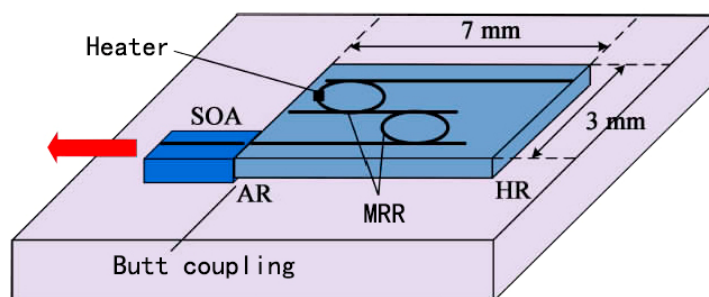


Figure 4. Structure diagram of double-MRR silicon substrate external cavity semiconductor laser.

In 2009, Takeshi Takeuchi et al. [13] reported the use of silicon waveguide (core material is SiON) three-MRR-and-SOA-integrated external cavity semiconductor laser, coupling SOA with silicon substrate through passive alignment technology, where the coupling mode is direct coupling. A waveguide reflector is used instead of high-reflection (HR) mirror to reduce the manufacturing cost. In the design of the microring structure, the threshold difference is fully considered, and the three-MRR structure is adopted. Compared with the two-MRR structure, the three-MRR structure has a larger threshold gain difference and can provide a more stable laser in a larger tuning range. The silicon-based external cavity semiconductor laser has a simple structure and is suitable for mass production. It has a

high fiber output power of more than 15 dBm, is able to tune wavelengths in the 60 nm range in the L-band, and contains 147 ITU-T channels with channel spacing of 50 GHz.

In the same year, Tao Chu et al. [14] proposed a silica-based external cavity tunable laser, which is mainly integrated through dual MRR and SOA. The structure is compact, and the size of the external cavity is only $0.7 \times 0.45 \text{ mm}^2$, about 1/25 of that of the traditional tunable laser. There is a wide tuning range, covering the optical communication C-band (1530–1565 nm) or L-band (1565–1610 nm), at the power of 26 mW, obtaining the maximum wavelength-tuning range of 38 nm.

Its structure is shown in Figure 5, consisting of an SOA and an external resonator. The resonator is made of silicon photonic line waveguide, and it is a double MRR. It is the first external cavity semiconductor laser made by silicon photonic technology. The ring resonator has a wide FSR due to its short cavity length. In addition, compared with the ring resonators made of SiON material, the ring resonators made of silicon photonic line waveguides have wider FSR due to their smaller bending radius of several microns. Therefore, the larger gain difference and wavelength-tuning range required for single-mode laser oscillation can be obtained more easily using a silicon ring resonator.

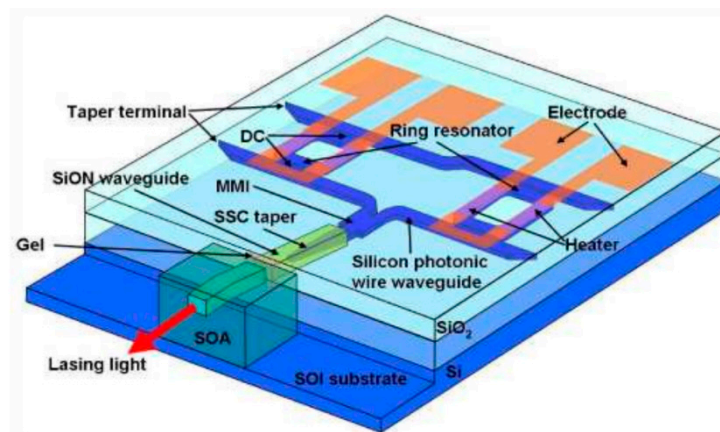


Figure 5. Structure of an external cavity tunable laser integrated with a silicon photonic line waveguide dual MRR and SOA.

In 2012, Keita Nemoto et al. [15] optimized the design of silicon substrate outer cavity semiconductor laser, using the ring resonator of silicon optical wire as the outer cavity, and produced a semiconductor laser with adjustable wavelength. The size of the ring resonator wavelength filter with outer cavity length of 6.0 mm is $1.78 \times 0.52 \text{ mm}^2$, which is about 1/8 of that of silicon (SiON) material. The maximum laser output power is 18.9 MW, using heating power of 115.7 mW and tuning operation of wavelength above 45.1 nm. The spectral linewidth of the whole L-band is less than 100 kHz, which is suitable for being used as the light source of the digital coherent light transmission system. The structure is shown in Figure 6.

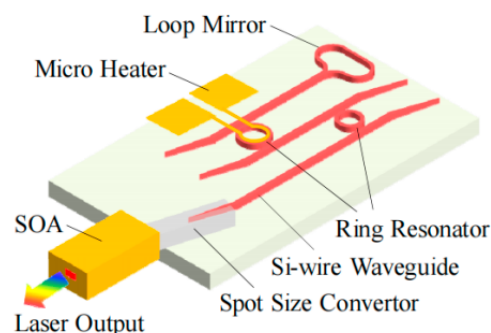


Figure 6. Schematic diagram of silicon photonic line waveguide ring cavity laser structure.

In 2013, Tomohiro Kita et al. [16] fabricated a tunable semiconductor laser with a maximum output power of 25.1 mW using a silicon photonic line waveguide ring resonator as an external optical cavity. The micro-heater can be continuously tuned to wavelengths above 50 nm, with a linewidth less than 100 kHz and a smaller size. While improving laser stability, it can be used in the actual digital coherent transmission system, as shown in Figure 7.

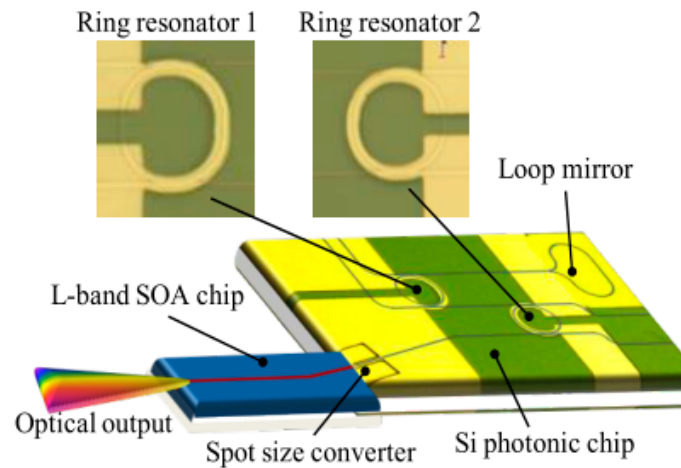


Figure 7. Schematic diagram of silicon-substrate tunable semiconductor laser.

In 2014, Sato et al. [17] integrated a silicon-based tunable filter, gain chip, and boost SOA, as shown in Figure 8. The tunable filter consists of two ring resonators, and the waveguide core of the gain part is composed of InGaAsP/InGaAsP base multiple quantum well. The laser side of the gain chip is coated with low-reflection (LR) coating and the output side of the boost SOA is coated with anti-reflection (AR) coating. The optical fiber coupling output power is greater than 100 mW, the linewidth is less than 15 kHz, the side-mode suppression ratio (SMSR) is greater than 45 dB, and the wavelength-tunable range is about 65 nm, enough to cover the entire C-band.

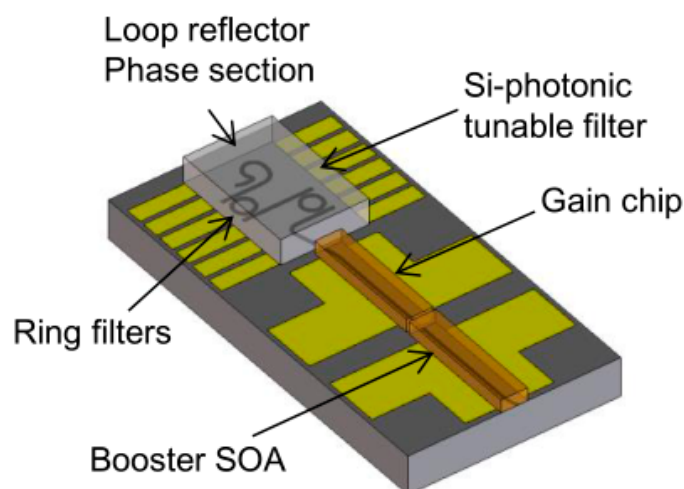


Figure 8. Schematic diagram of a silicon-photon mixed-ring external cavity tunable laser.

In 2015, Tin Komljenovic et al. [18] demonstrated a widely tunable external cavity semiconductor laser with an external cavity length of 4 cm through monolithic integration. The laser works in O-band and can be tuned in the range of 1237.7–1292.4 nm, with a tuning range of about 54 nm. Over the entire tuning range, SMSR is greater than 45 dB, output power is more than 10 mW, linewidth is less than 100 kHz, and the best single mode linewidth is 50 kHz.

In 2016, Zhao et al. [19] fabricated a low loss (0.1 dB/cm), high Q factor microring resonator based on double fringe SiN/SiO and developed a tunable InP/SiN mixed external cavity semiconductor laser, and the waveguide has good performance. The wavelength-tuning range of the laser is about 1530–1580 nm, the output power is 16 mW, the SMSR is more than 45 dB, and the linewidth is 65 kHz. It has broad application prospects in coherent transmission systems.

The schematic diagram of the laser is shown in Figure 9. It consists of a high-power InP/n-GaAsP SOA gain chip and two microring resonators. The front and back of the SOA are coated with highly reflective and AR coatings. Using the cursor effect, two MRR with slightly different radii are used to increase the wavelength-tuning range. Phase and power tuning sections are for fine-tuning longitudinal mode and output power, respectively.

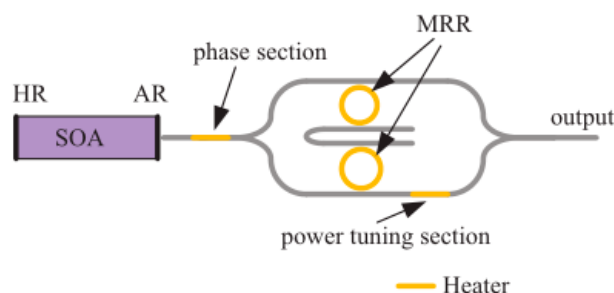


Figure 9. Schematic diagram of silicon-substrate MRR external cavity laser.

In 2017, Jing Zhang et al. [20] proposed a non-uniformly integrated, wide-tuned, unidirectional III–V ring laser on silicon. The wavelength-tuning range of the laser is 1560–1600 nm, and the ring radius of the ring resonator structure is 25 μm and 27 μm , respectively. The FSR in the wavelength range of 1550 nm is 4.1 nm and 3.7 nm, respectively. Using the Vernier effect of two ring resonators, a wide tuning range of 40 nm is obtained. Unidirectional operation is achieved throughout the tuning range, with a clockwise SMSR of about 10 dB. The linewidth is less than 1 MHz throughout the tuning range and can be reduced to 550 kHz at the optimal operating point.

In 2018, Hang Guan et al. [21] demonstrated a III–V/Si mixed external cavity laser with a tuning range greater than 60 nm, a maximum output power of 11 mW, a minimum linewidth of 37 kHz, a C-band that is always less than 80 kHz, a maximum SMSR of 55 dB, and a C-band that is always greater than 46 dB. It consists of a reflective external cavity constructed by RSOA, SSC, and a ring resonator.

In the same year, Minha Tran et al. [22] designed and manufactured a narrow-linewidth tuned laser with multi-ring mirrors. The structure is shown in Figure 10, including two-ring mirrors and three-ring mirrors. In heterogeneous silicon photons, a laser using a three-ring mirror was implemented, with an average SMSR of 55 dB in the 30 nm tuning range and a linewidth reduced to 17.5 kHz.

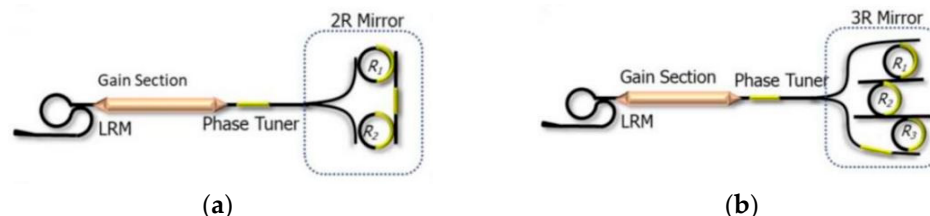


Figure 10. (a) Schematic diagram of a double-MRR tunable laser; (b) schematic diagram of a triple-MRR tunable laser.

In 2019, Yongkang Gao et al. [23] demonstrated a miniaturized packaged hybrid integrated silicon–photon (SiPh) tunable laser for coherent modules of small size. By integrating an internally designed high-power SOA, the SiPh laser developed achieved a record 21.5 dBm C-band output power with a linewidth of 60 kHz, an SMSR greater

than 50 dB, a relative intensity noise less than 150 dB/Hz, and a tuning range of 65 nm. In addition, frequency stability of the SiPh tunable laser at 1 GHz was achieved over the package temperature range from 10 °C to 80 °C and over SOA current variations of more than 200 mA, as shown in Figure 11.

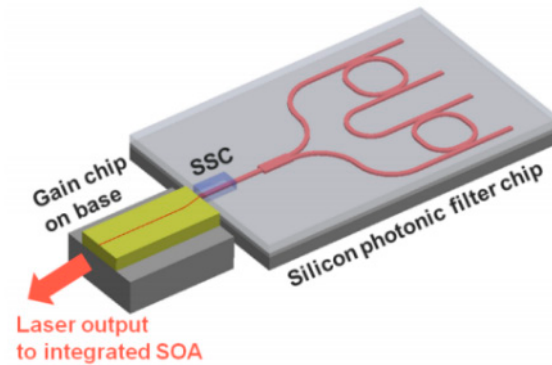


Figure 11. Schematic diagram of a hybrid integrated SiPh tunable laser.

In 2020, Jia Xu Brian Sia et al. [24] studied a cursors-based hybrid silicon–photonic tunable laser. By tuning the wavelength by MRR, the slope efficiency of the laser is 0.232 W/A, the output power is 28 mW, and the SMSR is 42 dB. When the thermal power of a single MRR reaches 47.2 mW, it can be tuned in the wavelength range of 1881–1947 nm, and the tuning range is 66 nm. In the same year, Jia Xu Brian Sia et al. [25] also reported a III–V/Si mixed wavelength-tunable laser with a working wavelength of 1647–1690 nm and a tuning range of 53 nm. Room-temperature continuous wave operation is realized, with output power up to 31.1 mW and corresponding maximum SMSR of 46.01 dB. The laser is hypercoherent with an estimated linewidth of 0.7 kHz, extending the coverage of the III–V/Si hybrid laser with a sub-kHz linewidth to the 1650 nm wavelength region beyond the L-band.

In 2021, Ruiling Zhao et al. [26] demonstrated a dual-gain InP–Si₃N₄ mixed external cavity laser, whose structure is shown in Figure 12. The working wavelength of the laser is 1550 nm, the tuning range is 44 nm of the working wavelength, the linewidth is 6.6 kHz, SMSR is greater than 67 dB, and the two gain parts work in parallel, thus providing high output power; the maximum power is about 23.5 mW.



Figure 12. Schematic structure of tunable InP–Si₃N₄ mixed external cavity laser with double parallel gain (the inset shows a cross-section of the Si₃N₄ waveguide).

In the same year, Yuyao Guo et al. [27] introduced a III–V /Si₃N₄ hybrid integrated laser with faster switching time, and its structure is shown in Figure 13. The working wavelength of the laser is 1516.5–1575 nm, the tuning range is 58.5 nm, the linewidth is 2.5 kHz, and the SMSR is greater than 70 dB. The maximum output power is 34 mW at 500 mA injection current.

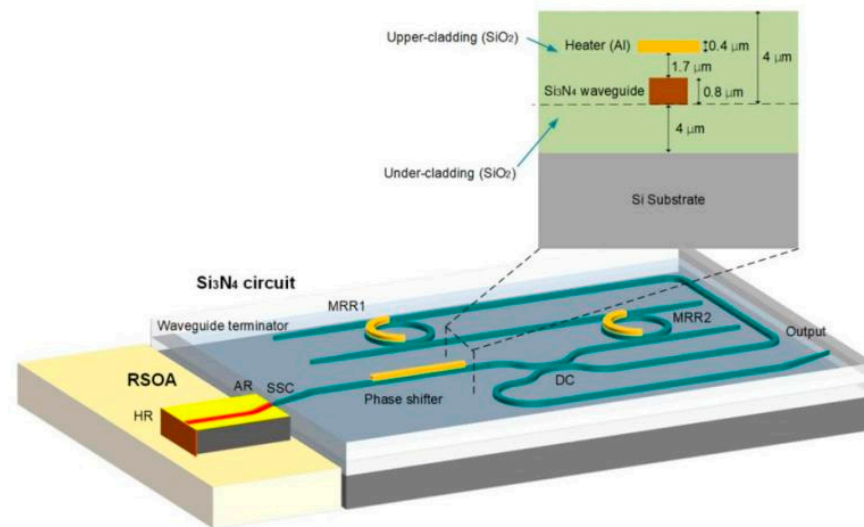


Figure 13. Schematic structure of the III-V/ Si_3N_4 hybrid laser (illustration shows a cross section of a thermally tunable Si_3N_4 waveguide).

3.2. MRR-and-MZI-Integrated External Cavity Semiconductor Lasers

The principle of how MZI works is shown in Figure 14. D1 and D2 are detectors, BS1 and BS2 are beam splitters, and M1 and M2 are mirrors. A beam splitter, BS1, splits an incoming monochromatic light beam from source S into two beams, which, after reflection by mirrors M1 and M2, recombine and interfere at BS2 to result in two outgoing beams (collected by detectors D1 and D2). When the phase along one of the paths varies, signals in both D1 and D2 oscillate out of phase, and as no photons are being lost, the sum of both signals stays always equal to the input, S.

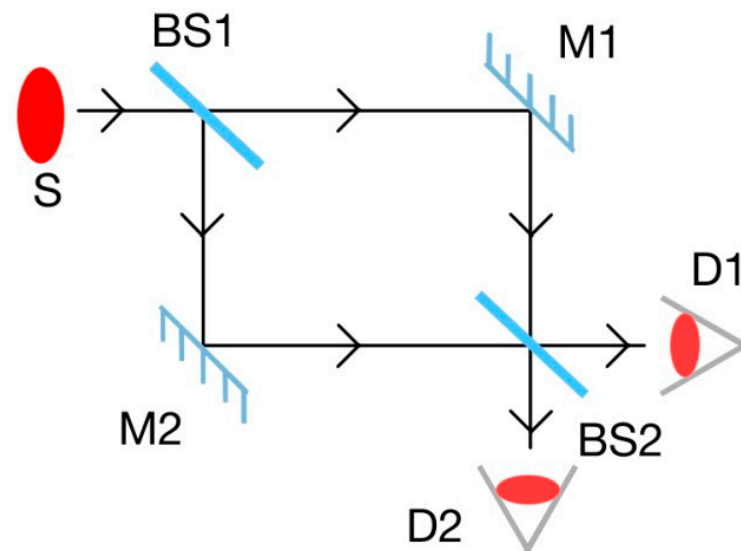


Figure 14. Principle of how MZI works.

In 2014, Debregeas et al. [28] proposed an integrated tunable laser that combines a reflective SOA (RSOA) with a silicon ring resonator-based outer cavity and MZI. The structure is shown in Figure 15. The external cavity of the laser is composed of two MRRs. The first ring is set to 25 GHz and the second ring is integrated with MZI.

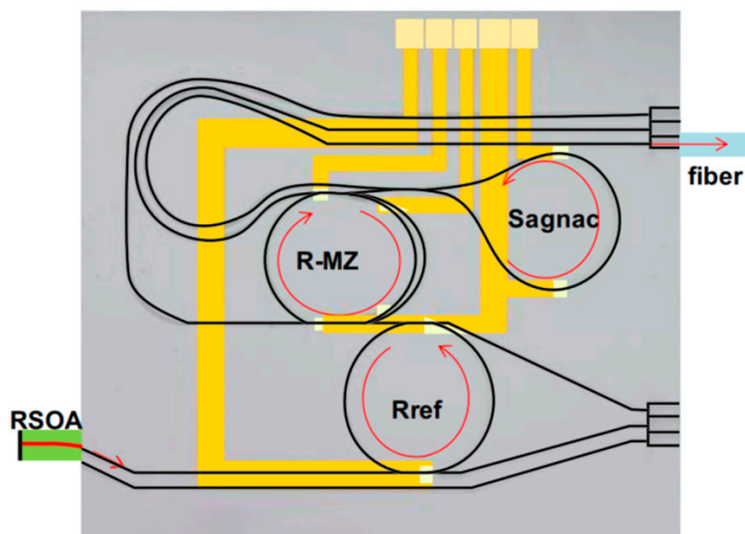


Figure 15. Structure diagram of RSOA and silicon substrate external cavity hybrid integrated laser.

In the same year, Tomohiro Kita et al. [29] fabricated a wavelength-tunable laser using a silicon photonic wavelength filter consisting of a ring resonator and an asymmetric MZI (A-MZI), as shown in Figure 16. The size, including the SOA, is very small, only $2.6 \times 0.5 \text{ mm}^2$, about 1/9 of the size of the silicon nitrous tunable laser. The wavelength-tuning range is more than $61.7 \pm 0.2 \text{ nm}$, covering the whole optical communication L-band, and SMSR is more than 38 dB. When the SOA injection current is 300 mA, the maximum optical output power is 42.2 mW, achieving a stable single-mode laser output. By optimizing the outer cavity design, a spectral linewidth of less than 100 kHz is obtained.

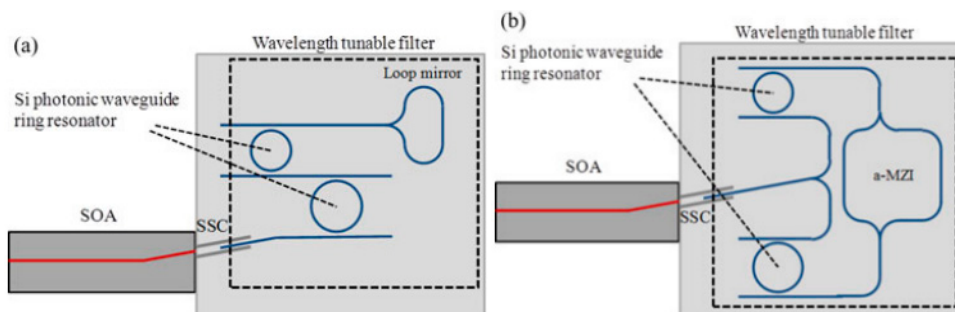


Figure 16. Schematic diagram of a wavelength-tunable silicon photon laser: (a) series configuration of ring resonators; (b) ring structure of ring resonators with A-MZI.

In 2015, Tomohiro Kita et al. [30] proposed a wavelength-tunable laser using silicon photonics to create a compact wavelength-tunable filter with high wavelength selectivity. Two ring resonators and A-MZI are used to realize a silicon photonic wavelength-tunable filter with a wide wavelength-tuning range. A wavelength-tunable laser made by docking a silicon photonic filter and an SOA achieved stable single-mode operation in a wide wavelength range. The size of the chip is $2.5 \times 0.6 \text{ mm}^2$, the laser threshold is 25 mA, the maximum fiber coupling output power is 8.9 mW, and the maximum output power is estimated to be 35 mW. The tuning wavelength range is 99.2 nm (1527.9–1627.1 nm), covering both C-band and L-band. Through the fine control of heating power, the side mode rejection ratio is greater than 29 dB.

Figure 17 is a schematic diagram of a silicon photonic tunable laser. The light from the SOA is filtered using two MRRs with slightly different FSRs and an A-MZI, and the FSR is about twice as large as the ring resonator FSRs. Laser wavelength is determined by the Vernier effect between two ring resonators. Wavelength selectivity is defined as

the transmittance difference between the main mode and the nearest mode. A large transmittance difference can achieve a stable single-mode laser.

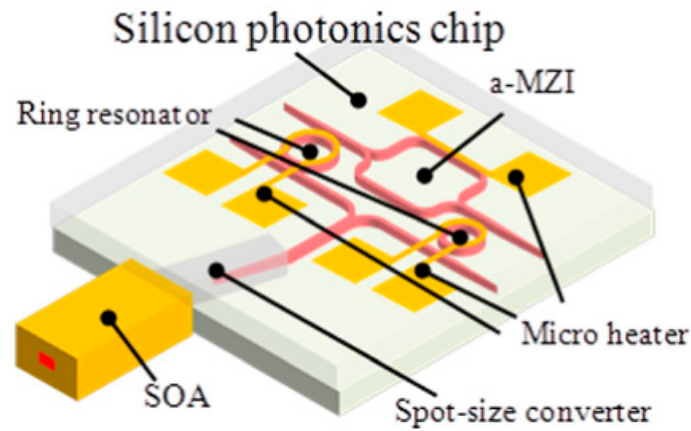


Figure 17. Schematic diagram of a silicon photonic tunable laser.

In the same year, Rui Tang et al. [31] proposed a narrow line-width silicon photonic tunable laser with a high A-MZI. The laser consists of two silicon ring resonators with different perimeters and a highly asymmetric MZI, with significantly different optical path lengths. The calculation and experimental results show that the high A-MZI increases the gain difference between the longitudinal modes. The result is a stable single-mode oscillation with a narrow band width of 12 kHz, which can be tuned in the wavelength range of 42.7 nm. The surface structure can also be applied to other ring resonator filters, regardless of the waveguide type.

The basic structure of the laser is shown in Figure 18. Both structures consist of an SOA and an external wavelength-tunable filter. SOA is a gain medium in C-band, and the filter consists of two ring resonators with different perimeters. The Vernier effect of two ring resonators is used to roughly select the oscillation wavelength.

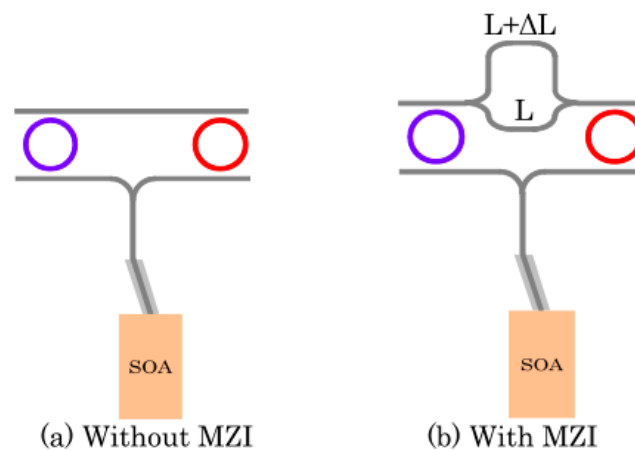


Figure 18. (a) Silicon-based laser without MZI. (b) Silicon-based laser with MZI.

In 2020, Aditya Malik et al. [32] proposed a widely tunable quantum dot laser heterointegrated on a silicon insulator substrate, and its structure is shown in Figure 19. The tuning mechanism is based on the Vernier double-ring geometry, and the tuning range is 47 nm at 52 dB SMSR. When the wavelength filter in the form of MZI is added to the cavity, the SMSR is increased to 58 dB, the tuning range is increased to 52 nm, and the linewidth is as low as 5.3 kHz.

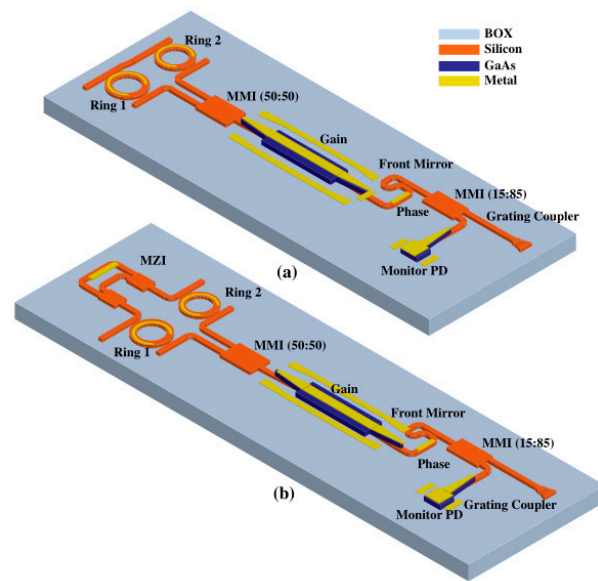


Figure 19. Schematic diagram of (a) and (b) double-ring cursors with MZI tunable lasers.

For Vernier ring lasers, the linewidth is in the range of 10–20 kHz, but due to the poor SMSR at the edge of the gain spectrum, the linewidth is as high as 50 kHz when the output wavelength is close to 1290 nm. When MZI is used, better SMSR can be obtained, so the linewidth is always less than 10 kHz in the total tuning range.

The research development on performance of SINLT-ECSLs in recent years is listed in Table 1. Compared with MRR-integrated external cavity semiconductor lasers, MRR-and-MZI-integrated external cavity semiconductor lasers have the characteristics of narrow-band filtering, which can minimize the transmittance of adjacent wavelengths at the maximum transmittance and improve the wavelength selectivity in the waveguide. By changing the temperature of the material through the micro-heater, the refractive index of the waveguide is changed, and wider wavelength-tuning range is realized. Therefore, MRR-and-MZI-integrated external cavity semiconductor lasers can make the lasers obtain narrower linewidth, wider wavelength-tuning range, and higher SMSR.

Table 1. A survey displaying developments in the field of the SINLT-ECSLs.

Laser Type	Band	λ (nm)	Tuning Range (nm)	Linewidth (kHz)	SMSR (dB)	Output Power		Year
						mW	dBm	
MRR	C, L	-	45.2	-	>45	>2.9 *	>4.7	2006 [12]
MRR	C, L	1540–1636	96	-	>50	>20 *	>13	2009 [13]
MRR	C, L	1530–1610	38	-	>30	26	14.1 *	2009 [14]
MRR	L	-	45.1	<100	>40	18.9	12.8 *	2012 [15]
MRR	L	-	53	<100	>25	25.1	14 *	2013 [16]
MRR	C, L	1510–1575	65	<15	>45	>100 *	>20	2014 [17]
MRR and MZI	C, L	-	35	2	>60	3.2 *	5	2014 [28]
MRR and MZI	L	-	61.7±0.2	<100	>38	42.2	16.3 *	2014 [29]
MRR	O	1237.7–1292.4	54.7	<100	>45	10	10 *	2015 [18]
MRR and MZI	C, L	1527.9–1627.1	99.2	-	>29	35	15.4 *	2015 [30]
MRR and MZI	C, L	-	42.7	12	-	30	14.8 *	2015 [31]
MRR	C, L	1530–1580	50	65	>45	16	12 *	2016 [19]
MRR	C, L	1560–1600	40	<1000	10	>1.4 *	>1.5	2017 [20]

Table 1. Cont.

Laser Type	Band	λ (nm)	Tuning Range (nm)	Linewidth (kHz)	SMSR (dB)	Output Power		Year
						mW	dBm	
MRR	C	-	60	<80	>46	11	10.4 *	2018 [21]
MRR	C, L	1557–1587	30	17.5	>55	6.9	8.4 *	2018 [22]
MRR	C	-	65	60	>50	141.3 *	21.5	2019 [23]
MRR	-	1881–1947	66	-	42	28	14.5 *	2020 [24]
MRR	-	1647–1690	43	0.7	46	31.1 *	14.9	2020 [25]
MRR and MZI	O	-	52	5.3	58	10	10 *	2020 [32]
MRR	C, L	1524–1568	44	6.6	>67	23.5 *	13.7	2021 [26]
MRR	C, L	1516.5–1575	58.5	2.5	>70	34 *	15.3	2021 [27]

Legend: *—Calculated.

4. Integration of SINLT-ECSLs

4.1. Monolithic Integrated

Monolithic integration mainly refers to the direct epitaxial growth of group III–V compound semiconductor materials on the silicon substrate and synchronous device fabrication process. Due to the high-density thread dislocation in heteroepitaxy, the laser device performance and reliability will be poor due to the direct growth on silicon [33]. However, the gain characteristics can be fine-tuned by changing the growth conditions, so that the device has a long life even when it is epitaxial grown on silicon with high dislocation density [34]. For example, Chen et al. realized high-performance quantum dot lasers on silicon by combining the nucleation layer and dislocation filter layer with in situ thermal annealing and adopting the molecular beam epitaxy (MBE) epitaxial growth method to achieve high-quality GaAs-on-Si layer with low defects. The large lattice mismatch between III–V materials and silicon is no longer an obstacle to the single epitaxial growth of III–V photonic devices on silicon substrates, demonstrating the ability to grow uniformly high-quality III–V materials on the entire Si substrate, which is a significant advance in silicon-based photonics and optoelectronics integration [35].

In 2020, Bahawal Haq et al. [36] produced a C-band monolithic integration laser; its structure is shown in Figure 20. At 20 °C, the threshold current of 80 mA and the maximum single-waveguide coupled output power exceeding 6.9 mW are obtained, with the slope efficiency of 0.27 W/A and the SMSR greater than 33 dB.

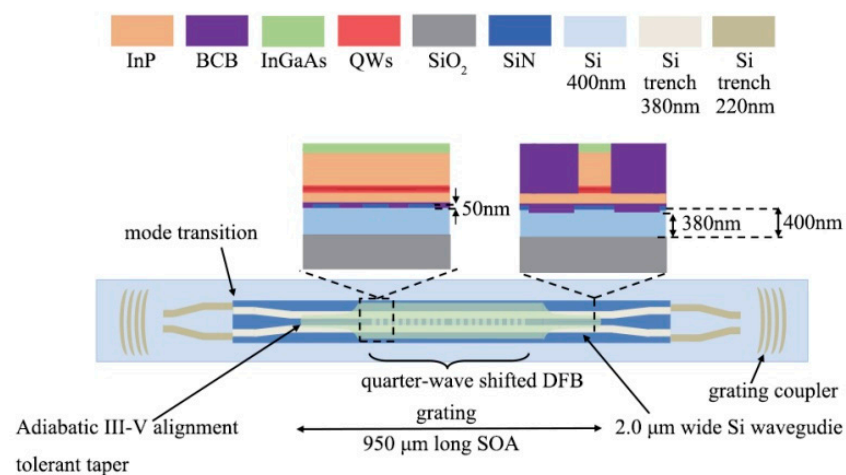


Figure 20. Schematic structure of monolithic integration laser.

4.2. Heterogeneous Integration

Heterointegration [37] refers to the integration of an epitaxial growth group III–V compound semiconductor with silicon substrate through bonding technology, and then the device manufacturing process. Bonding can be divided into direct bonding, adhesive bonding, and metal bonding. Similar to hybrid integration, heterogeneous integration has the advantage of selecting the best materials for each function (i.e., lasers, low-loss waveguides, detectors), resulting in highly complex photonic integrated circuits (PIC). Thus, heterogeneous integration has all the scaling advantages of monolithic integration, while gaining greater flexibility in material selection, resulting in superior performance. However, because the output power of heterogeneous integration is relatively low, it cannot be well applied in multi-channel communication, and the whole processing process is complicated, the bonding repetition rate is not high, and it is difficult to carry out large-scale mass production.

In 2018, Sulakshna Kumari et al. [38] designed a heterogeneously integrated continuous-wave electrically-pumped vertical-cavity Si-integrated laser (VCSIL). Its structure is shown in Figure 21. The VCSIL structure consists of two distinct parts, called the upper half and the lower half. The upper part of the structure is a semi-vertical cavity surface-emitting laser based on GaAs, oxide layer, DBR, and gold film. The lower part of the structure is a SiN waveguide/dielectric DBR combination on a silicon substrate. SiO₂ cladding at the top and bottom prevents the waveguide mode from leaking into the high-refractive-index GaAs semi-vertical cavity surface-emitting laser and the high-refractive-index dielectric DBR and Si substrates. A VCSIL with a 5 μm oxide aperture diameter has a threshold current of 1.13 mA and produces a maximum single-sided waveguide coupled output power of 73 μW at 856 nm. The slope efficiency and the thermal impedance of the corresponding device is 0.085 W/A and 11.8 K/mW, respectively. The SMSR is 29 dB at a bias current of 2.5 mA.

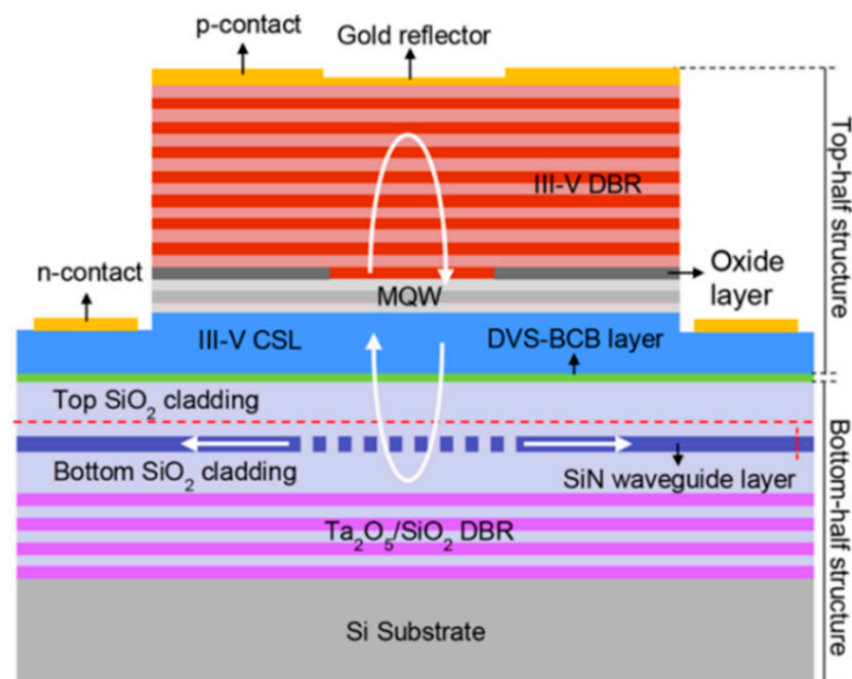


Figure 21. Schematic cross-section of heterogeneously integrated VCSIL.

In 2020, Chao Xiang et al. [39] designed a multilayer heterointegrated III–V/Si/Si₃N₄ laser structure, which can achieve a high-efficiency electro-pumped laser in a fully integrated Si₃N₄-based outer cavity. The structure is shown in Figure 22. The linewidth of the laser is 6 kHz, and it has good temperature stability and low phase noise. The Si₃N₄ spiral

grating provides a narrowband filter together with high extinction ratio. This results in a large lasing SMSR of over 58 dB.

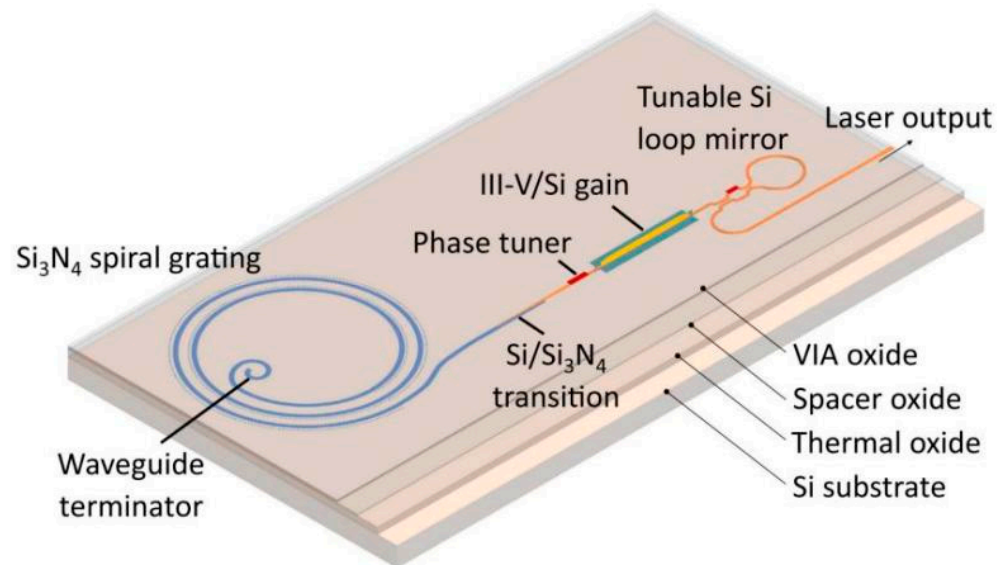


Figure 22. Schematic structure of hetero integrated laser.

4.3. Hybrid Integrated

Hybrid integration refers to the integrated assembly of the III–V laser chip and silicon substrate. These can be achieved with prior technology, but there is a drawback that two devices of different sizes or materials must be aligned to sub-micron accuracy for effective coupling [40]. However, it can also be improved in certain ways to avoid defects as much as possible. For example, Alexander W. Fang et al. [41] designed a special structure that can be performed at the wafer, partial wafer, or wafer level so that multiple lasers do not require any critical alignment of the silicon waveguide with III–V materials. In addition, this highly scalable structure can be extended to other active devices on silicon, such as optical amplifiers, modulators, and optical detectors, by selectively changing the III–V structure through processes such as quantum well mixing or non-planar wafer bonding.

In 2020, Yeyu Zhu et al. [42] designed the hybrid integration of low-loss passive Si_3N_4 outer cavity and $1.3\ \mu\text{m}$ quantum dot RSOA, and its structure is shown in Figure 23. Chip-scale, tunable, narrow-linewidth hybrid-integrated diode lasers based on quantum-dot RSOAs at $1.3\ \mu\text{m}$ are demonstrated through butt-coupling to a silicon–nitride photonic integrated circuit. The hybrid laser linewidth is around 85 kHz, and the tuning range is around 47 nm.

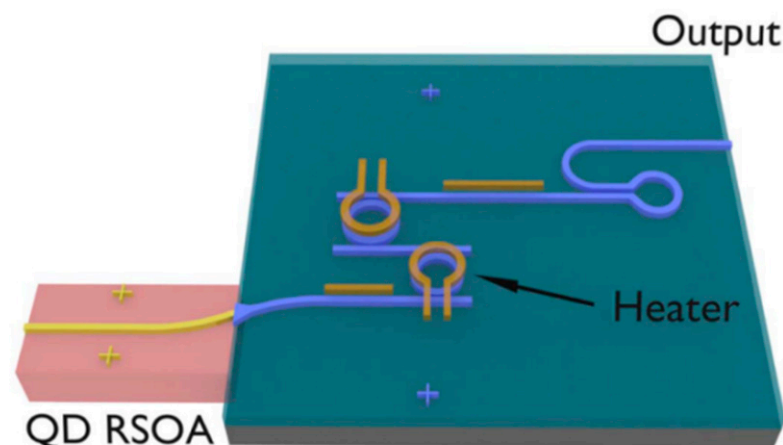


Figure 23. Schematic structure of hybrid-integrated laser.

In 2021, Yilin Xu et al. [43] designed a new hybrid-integrated laser, with the structure shown in Figure 24. The device consists of an InP-based RSOA that is connected to a thermally tunable feedback circuit on a silicon photonic (SiP) chip. A photonic wire bond connects the facet of the RSOA to the SiP external-cavity feedback circuit. The assembly is built on a metal submount that simultaneously acts as an efficient heat sink. The photonic wire bonding can be written in situ in a fully automated process and is shaped to fit the size of the mode field and the positions of the chips at both ends, thus providing low loss coupling even with limited placement accuracy. It demonstrates a tuning range from 1515 to 1565 nm along with side-mode suppression ratios above 40 dB and intrinsic linewidths down to 105 kHz. The approach combines the scalability advantages of monolithic integration with the performance and flexibility of hybrid multi-chip assemblies and may thus open a path towards integrated external cavity semiconductor lasers on a wide variety of integration platforms.

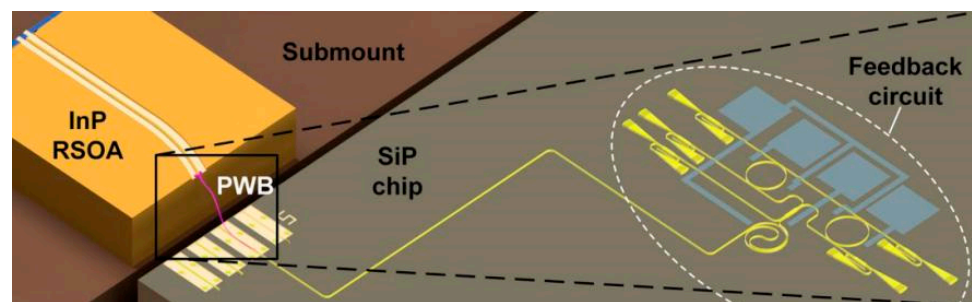


Figure 24. Schematic structure of hybrid-integrated laser using photonic line bonds as intracavity coupling elements.

5. Conclusions

SINLT-ECSLs are developing towards wider tuning range, narrower linewidth, and higher side-mode rejection ratio. Through the selection of gain media, materials, integrated devices, etc., and the design of new silicon-based outer cavity structure, the epitaxial design of SOA is improved, the loss of silicon waveguide is reduced [44], the coupling efficiency is increased, the reflectivity is reduced, and the stability is enhanced, so as to meet the application requirements in various fields. High-performance silicon-based external cavity semiconductor lasers with narrow linewidth or even ultra-narrow linewidth, wide tuning range, stable output, low noise, small volume, and low cost are realized. With the development of the information age, silicon-based external cavity semiconductor lasers will have a broader application market in optical communication, coherent detection, and other fields [45]. How to realize wide tuning range, high power, single mode, stable spectral output, and high SMSR laser output is a main research direction for the future development of external cavity semiconductor lasers.

In summary, the advantages of the SINLT-ECSLs over solitary diode lasers are so important that their future looks encouraging. This conclusion becomes still better supported if we consider multichannel external cavity lasers that are particularly interesting for optical interconnection applications. New materials and configurations appear that make these lasers still more attractive due to extension of the operation spectral range and high power. Last, but not least, the SINLT-ECSLs have the potential to be fabricated cheaply enough to promote more applications.

Author Contributions: Conceptualization, X.L. and J.S.; methodology, K.D. and Y.M.; writing—original draft preparation, X.L. and Z.L.; writing—review and editing, L.W., L.L. and L.Z.; visualization, Y.Q., Z.Q. and G.L.; supervision, Z.Q.; funding acquisition, G.L. All authors have read and agreed to the published version of the manuscript.

Funding: This work was supported in part by the Major Science and Technology Program of Hainan Province of China under Grant ZDKJ2019005; in part by Scientific Research Projects of Higher Ed-

education Institutions in Hainan Province under Grant hnky2020-24, Grant Hnjg2021ZD-22, Grant hnky2020ZD-12; in part by the Hainan Provincial Natural Science Foundation of China under Grant 120MS031, Grant 2019RC190, Grant 2019RC192; in part by the Special Research Project of Hainan Academician Innovation Platform under Grant SPTZX202034; in part by the National Natural Science Foundation of China under Grant 61774024, Grant 61864002, Grant 11764012, Grant 62174046, Grant 62064004 and Grant 61964007; in part by the Key Research and Development Projects in Hainan Province under Grant ZDYF2020020, Grant ZDYF2020036, and Grant ZDYF2020217; in part by specific research fund for Innovation Platform for Academicians of Hainan Province under Grant YSPTZX202034 and Grant YSPTZX202127; in part by Open Fund for Innovation and Entrepreneurship of college students under Grant 202111658021X, Grant 202111658022X, Grant 202111658023X, Grant 202111658013.

Institutional Review Board Statement: Not applicable.

Informed Consent Statement: Not applicable.

Data Availability Statement: Not applicable.

Acknowledgments: The authors thank Dongxin Xu, Hao Chen, and Yanbo Liang for helping with this article.

Conflicts of Interest: The authors declare no conflict of interest.

References

1. Verdier, A.; de Valicourt, G.; Brenot, R.; Debregeas, H.; Dong, P.; Earnshaw, M.; Carrère, H.; Chen, Y. Ultrawideband wavelength-tunable hybrid external-cavity lasers. *J. Lightwave Technol.* **2017**, *36*, 37–43. [[CrossRef](#)]
2. Tran, M.A.; Huang, D.; Guo, J.; Komljenovic, T.; Morton, P.A.; Bowers, J.E. Ring-resonator based widely-tunable narrow-linewidth Si/InP integrated lasers. *IEEE J. Sel. Top. Quantum Electron.* **2019**, *26*, 1500514. [[CrossRef](#)]
3. Zhu, Y.; Zhu, L. Narrow-linewidth, tunable external cavity dual-band diode lasers through InP/GaAs-Si₃N₄ hybrid integration. *Opt. Express* **2019**, *27*, 2354–2362. [[CrossRef](#)] [[PubMed](#)]
4. Malik, A.; Xiang, C.; Chang, L.; Jin, W.; Guo, J.; Tran, M.; Bowers, J. Low noise, tunable silicon photonic lasers. *Appl. Phys. Rev.* **2021**, *8*, 031306. [[CrossRef](#)]
5. Liang, W.; Ilchenko, V.S.; Eliyahu, D.; Savchenkov, A.A.; Matsko, A.B.; Seidel, D.; Maleki, L. Ultralow noise miniature external cavity semiconductor laser. *Nat. Commun.* **2015**, *6*, 7371. [[CrossRef](#)]
6. Suzuki, K.; Kita, T.; Yamada, H. Wavelength tunable laser diodes with Si-wire waveguide ring resonator wavelength filters. In *Silicon Photonics VI*; International Society for Optics and Photonics: San Francisco, CA, USA, 2011; Volume 7943.
7. Bowers, J.E.; Komljenovic, T.; Srinivasan, S.; Hulme, J.; Davenport, M. A comparison of widely tunable, narrow linewidth ring cavity lasers on silicon substrates. In Proceedings of the 2015 IEEE Photonics Conference (IPC), Reston, VA, USA, 4–8 October 2015; pp. 533–534.
8. Lee, J.; Bovington, J.; Shubin, I.; Luo, Y.; Yao, J.; Lin, S.; Cunningham, J.E.; Raj, K.; Krishnamoorthy, A.V.; Zheng, X. 12.2% waveguide-coupled wall plug efficiency in single mode external-cavity tunable Si/III–V hybrid laser. In Proceedings of the 2015 IEEE Optical Interconnects Conference (OI), San Diego, CA, USA, 20–22 April 2015; pp. 142–143.
9. Srinivasan, S.; Davenport, M.; Komljenovic, T.; Hulme, J.; Spencer, D.T.; Bowers, J.E. Coupled-ring-resonator-mirror-based heterogeneous III–V silicon tunable laser. *IEEE Photonics J.* **2015**, *7*, 2700908. [[CrossRef](#)]
10. Wang, R.; Sprengel, S.; Vasiliev, A.; Boehm, G.; van Campenhout, J.; Lepage, G.; Verheyen, P.; Baets, R.; Amann, M.; Roelkens, G. Widely tunable 2.3 μm III–V-on-silicon Vernier lasers for broadband spectroscopic sensing. *Photonics Res.* **2018**, *6*, 858–866. [[CrossRef](#)]
11. Hulme, J.C.; Doylend, J.K.; Bowers, J.E. Widely tunable Vernier ring laser on hybrid silicon. *Opt. Express* **2013**, *21*, 19718–19722. [[CrossRef](#)]
12. Ishizaka, M.; Yamazaki, H. Wavelength tunable laser using silica double ring resonators. *Electron. Commun. Jpn.* **2006**, *89*, 34–41. [[CrossRef](#)]
13. Takeuchi, T.; Takahashi, M.; Suzuki, K.; Watanabe, S.; Yamazaki, H. Wavelength tunable laser with silica-waveguide ring resonators. *IEICE Trans. Electron.* **2009**, *92*, 198–204. [[CrossRef](#)]
14. Chu, T.; Fujioka, N.; Ishizaka, M. Compact, lower-power-consumption wavelength tunable laser fabricated with silicon photonic wire waveguide micro-ring resonators. *Opt. Express* **2009**, *17*, 14063–14068. [[CrossRef](#)] [[PubMed](#)]
15. Nemoto, K.; Kita, T.; Yamada, H. Narrow spectral linewidth wavelength tunable laser with Si photonic-wire waveguide ring resonators. In Proceedings of the 9th International Conference on Group IV Photonics (GFP), San Diego, CA, USA, 29–31 August 2012; pp. 216–218.
16. Kita, T.; Nemoto, K.; Yamada, H. Narrow spectral linewidth and high output power Si photonic wavelength tunable laser diode. In Proceedings of the 10th International Conference on Group IV Photonics, Seoul, Korea, 28–30 August 2013; pp. 152–153.

17. Kobayashi, N.; Sato, K.; Namiwaka, M.; Yamamoto, K.; Watanabe, S.; Kita, T.; Yamada, H.; Yamazaki, H. Silicon photonic hybrid ring-filter external cavity wavelength tunable lasers. *J. Lightwave Technol.* **2015**, *33*, 1241–1246. [[CrossRef](#)]
18. Komljenovic, T.; Srinivasan, S.; Norberg, E.; Davenport, M.; Fish, G.; Bowers, J.E. Widely tunable narrow-linewidth monolithically integrated external-cavity semiconductor lasers. *IEEE J. Sel. Top. Quantum Electron.* **2015**, *21*, 214–222. [[CrossRef](#)]
19. Zhao, J.L.; Oldenbeuving, R.M.; Epping, J.P.; Hoekman, M.; Heideman, R.G.; Dekker, R.; Fan, Y.; Boller, K.-J.; Ji, R.Q.; Fu, S.M.; et al. Narrow-linewidth widely tunable hybrid external cavity laser using Si₃N₄/SiO₂ microring resonators. In Proceedings of the 2016 IEEE 13th International Conference on Group IV Photonics (GFP), Shanghai, China, 24–26 August 2016; pp. 24–25.
20. Zhang, J.; Li, Y.; Dhoore, S.; Morthier, G.; Roelkens, G. Unidirectional, widely-tunable and narrow-linewidth heterogeneously integrated III-V-on-silicon laser. *Opt. Express.* **2017**, *25*, 7092–7100. [[CrossRef](#)]
21. Guan, H.; Novack, A.; Galfsky, T.; Ma, Y.; Fatholouloumi, S.; Horth, A.; Huynh, T.N.; Roman, J.; Shi, R.; Caverley, M.; et al. Widely-tunable, narrow-linewidth III-V/silicon hybrid external-cavity laser for coherent communication. *Opt. Express* **2018**, *26*, 7920–7933. [[CrossRef](#)]
22. Tran, M.A.; Huang, D.; Komljenovic, T.; Liu, S.; Liang, L.; Kennedy, M.J.; Bowers, J.E. Multi-ring mirror-based narrow-linewidth widely-tunable lasers in heterogeneous silicon photonics. In Proceedings of the 2018 European Conference on Optical Communication (ECOC), Rome, Italy, 23–27 September 2018.
23. Gao, Y.; Lo, J.; Lee, S.; Patel, R.; Zhu, L.; Nee, J.; Tsou, D.; Carney, R.; Sun, J. High-power, narrow-linewidth, miniaturized silicon photonic tunable laser with accurate frequency control. *J. Lightwave Technol.* **2020**, *38*, 265–271. [[CrossRef](#)]
24. Sia, J.X.B.; Wang, W.; Qiao, Z.; Li, X.; Guo, T.X.; Zhou, J.; Littlejohns, C.G.; Liu, C.; Reed, G.T.; Wang, H. Analysis of Compact Silicon Photonic Hybrid Ring External Cavity (SHREC) Wavelength-Tunable Laser Diodes Operating From 1881–1947 nm. *IEEE J. Quantum Electron.* **2020**, *56*, 2001311. [[CrossRef](#)]
25. Sia, J.X.B.; Li, X.; Wang, W.; Qiao, Z.; Guo, X.; Zhou, J.; Littlejohns, C.G.; Liu, C.; Reed, G.T.; Wang, H. Sub-kHz linewidth, hybrid III-V/silicon wavelength-tunable laser diode operating at the application-rich 1647–1690 nm. *Opt. Express* **2020**, *28*, 25215–25224.
26. Zhao, R.; Guo, Y.; Lu, L.; Nisar, M.S.; Chen, J.; Zhou, L. Hybrid dual-gain tunable integrated InP-Si₃N₄ external cavity laser. *Opt. Express* **2021**, *29*, 10958–10966. [[CrossRef](#)]
27. Guo, Y.; Zhao, R.; Zhou, G.; Lu, L.; Stroganov, A.; Nisar, M.S.; Chen, J.; Zhou, L. Thermally Tuned High-Performance III-V/Si₃N₄ External Cavity Laser. *IEEE Photonics J.* **2021**, *13*, 1500813. [[CrossRef](#)]
28. Debregeas, H.; Ferrari, C.; Cappuzzo, M.A.; Klemens, F.; Keller, R.; Pardo, F.; Bolle, C.; Xie, C.; Earnshaw, M.P. 2kHz linewidth C-band tunable laser by hybrid integration of reflective SOA and SiO₂ PLC external cavity. In Proceedings of the 2014 International Semiconductor Laser Conference, Palma de Mallorca, Spain, 7–10 September 2014; pp. 50–51.
29. Kita, T.; Nemoto, K.; Yamada, H. Silicon photonic wavelength-tunable laser diode with asymmetric Mach–Zehnder interferometer. *IEEE J. Sel. Top. Quantum Electron.* **2013**, *20*, 344–349. [[CrossRef](#)]
30. Kita, T.; Tang, R.; Yamada, H. Compact silicon photonic wavelength-tunable laser diode with ultra-wide wavelength tuning range. *Appl. Phys. Lett.* **2015**, *106*, 111104. [[CrossRef](#)]
31. Tang, R.; Kita, T.; Yamada, H. Narrow-spectral-linewidth silicon photonic wavelength-tunable laser with highly asymmetric Mach–Zehnder interferometer. *Opt. Lett.* **2015**, *40*, 1504–1507. [[CrossRef](#)] [[PubMed](#)]
32. Malik, A.; Guo, J.; Tran, M.A.; Kurczveil, G.; Liang, D.; Bowers, J.E. Widely tunable, heterogeneously integrated quantum-dot O-band lasers on silicon. *Photonics Res.* **2020**, *8*, 1551–1557. [[CrossRef](#)]
33. Liu, A.Y.; Zhang, C.; Norman, J.; Snyder, A.; Lubyshev, D.; Fastenau, J.M.; Liu, A.W.K.; Gossard, A.C.; Bowers, J.E. High performance continuous wave 1.3 μm quantum dot lasers on silicon. *Appl. Phys. Lett.* **2014**, *104*, 041104. [[CrossRef](#)]
34. Norman, J.C.; Jung, D.Z.Z.; Wan, Y.; Liu, S.; Shang, C.; Herrick, R.W.; Chow, W.W.; Gossard, A.C.; Bowers, J.E. A review of high-performance quantum dot lasers on silicon. *IEEE J. Quantum Electron.* **2019**, *55*, 2000511. [[CrossRef](#)]
35. Chen, S.; Li, W.; Wu, J.; Jiang, Q.; Tang, M.; Shutts, S.; Elliott, S.N.; Sobiesierski, A.; Seeds, A.J.; Ross, I.; et al. Electrically pumped continuous-wave III–V quantum dot lasers on silicon. *Nat. Photonics* **2016**, *10*, 307–311. [[CrossRef](#)]
36. Haq, B.; Vaskasi, J.R.; Zhang, J.; Gocalinska, A.; Pelucchi, E.; Corbett, B.; Roelkens, G. Micro-transfer-printed III-V-on-silicon C-band distributed feedback lasers. *Opt. Express* **2020**, *28*, 32793–32801. [[CrossRef](#)] [[PubMed](#)]
37. Grund, D.W.; Ejzak, G.A.; Schneider, G.J.; Murakowski, J.; Prather, D.W. Heterogeneous integrated silicon-photonics module for producing widely tunable narrow linewidth RF. In Proceedings of the 2013 IEEE International Topical Meeting on Microwave Photonics (MWP), Alexandria, VA, USA, 28–31 October 2013; pp. 100–103.
38. Kumari, S.; Haglund, E.P.; Gustavsson, J.S.; Larsson, A.; Roelkens, G.; Baets, R.G. Vertical-Cavity Silicon-Integrated Laser with In-Plane Waveguide Emission at 850 nm. *Laser Photonics Rev.* **2018**, *12*, 1700206. [[CrossRef](#)]
39. Xiang, C.; Jin, W.; Guo, J.; Peters, J.D.; Kennedy, M.J.; Selvidge, J.; Morton, P.A.; Bowers, J.E. Narrow-linewidth III-V/Si/Si₃N₄ laser using multilayer heterogeneous integration. *Optica* **2020**, *7*, 20–21. [[CrossRef](#)]
40. Fan, Y.; Oldenbeuving, R.M.; Klein, E.J.; Lee, C.J.; Song, H.; Khan, M.R.H.; Offerhaus, H.L.; Van der Slot, P.J.M.; Boller, K.J. A hybrid semiconductor-glass waveguide laser. In *Laser Sources and Applications II*; International Society for Optics and Photonics: Brussels, Belgium, 2004; Volume 9135, pp. 231–236.
41. Fang, A.W.; Park, H.; Cohen, O.; Jones, R.; Panizza, M.J.; Bowers, J.E. Electrically pumped hybrid AlGaInAs-silicon evanescent laser. *Opt. Express* **2006**, *14*, 9203–9210. [[CrossRef](#)] [[PubMed](#)]
42. Zhu, Y.; Zeng, S.; Zhu, L. Optical beam steering by using tunable, narrow-linewidth butt-coupled hybrid lasers in a silicon nitride photonics platform. *Photonics Res.* **2020**, *8*, 375–380. [[CrossRef](#)]

43. Xu, Y.; Maier, P.; Blaicher, M.; Dietrich, P.; Marin-Palomo, P.; Hartmann, W.; Bao, Y.; Peng, H.; Billah, M.R.; Singer, S.; et al. Hybrid external-cavity lasers (ECL) using photonic wire bonds as coupling elements. *Sci. Rep.* **2021**, *11*, 16426. [[CrossRef](#)] [[PubMed](#)]
44. Stern, B.; Ji, X.; Dutt, A.; Lipson, M. Compact narrow-linewidth integrated laser based on a low-loss silicon nitride ring resonator. *Opt. Lett.* **2017**, *42*, 4541–4544. [[CrossRef](#)]
45. Kita, T.; Tang, R.; Yamada, H. Narrow spectral linewidth silicon photonic wavelength tunable laser diode for digital coherent communication system. *IEEE J. Sel. Top. Quantum Electron.* **2016**, *22*, 23–34. [[CrossRef](#)]